Multi-scale water balance analysis of a thawing boreal peatland complex near the southern permafrost limit in western Canada

Alexandre Lhosmot[1*], Gabriel Hould Gosselin[1,2*], Manuel Helbig[1,3], Julien Fouché[1,4], Youngryel Ryu[5], Matteo Detto[6], Ryan Connon[7], William Quinton[8], Tim Moore[9] and Oliver Sonnentag[1, 10]

[1]Département de géographie, Université de Montréal, Montréal, QC, Canada
[2]Department of Geography and Environmental Sciences, Northumbria University, Newcastle upon Tyne, UK
[3]Department of Physics & Atmospheric Science, Dalhousie University, Halifax, NS, Canada
[4]LISAH, Université de Montpellier, INRAE, IRD, Institut Agro, AgroParisTech, Montpellier, France
[5]Department of Landscape Architecture and Rural Systems Engineering, Seoul National University, Seoul, South Korea
[6]Department of Ecology and Evolutionary Biology, Princeton University, Princeton, NJ, USA
[7]Environment and Climate Change, Government of the Northwest Territories, Yellowknife, NT, Canada
[8]Cold Regions Research Centre, Wilfrid Laurier University, Waterloo, ON, Canada
[9]Department of Geography, McGill University, Montréal, QC, Canada
[10]Department of Geography and Environmental Studies, Wilfrid Laurier University, Waterloo, ON, Canada

[*]These authors share the co-first authorship.

Correspondence to: Alexandre Lhosmot (alexandrelhosmot@gmail.com) and Oliver Sonnentag (oliver.sonnentag@umontreal.ca)

Supplementary figures

Figures S1: Cutthroat flume installed at the West sub-basin outlet West1 in a) 2014 (i.e., before the late-season wildfire in October 2022), and b) 2024 (i.e., after the late-season wildfire in October 2022).

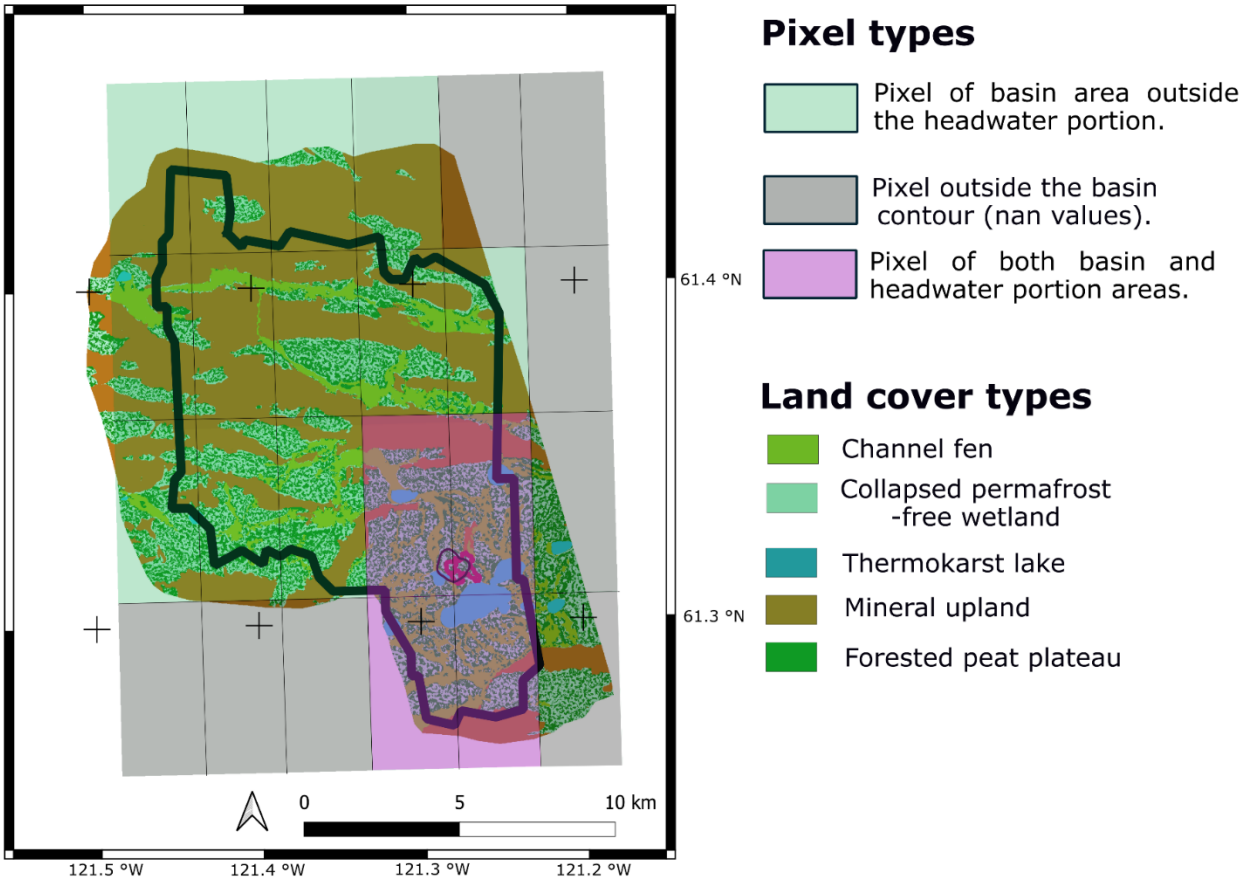

Figure S2: Location and description of the pixels (0.05 degrees of resolution) used for estimating ET with the Breathing Earth System Simulator (BESS) model (Jiang et al., 2016). The landscape map was produced by Chasmer et al. (2014). The black contour corresponds to the basin boundaries derived-from the SRTM DEM (130 km²).

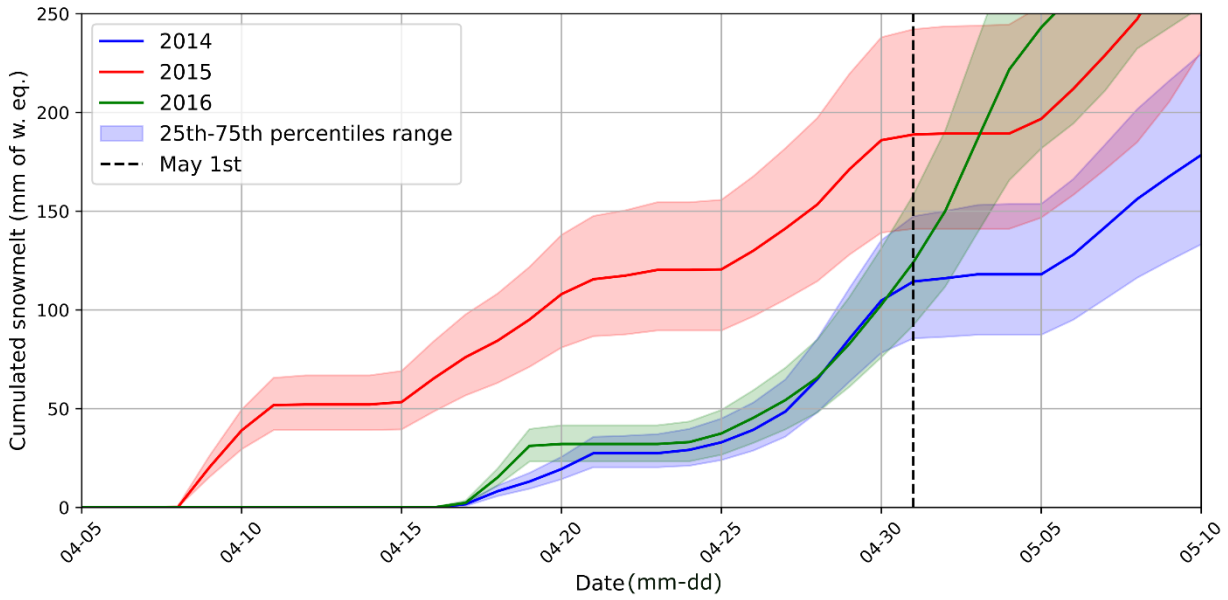

Figure S3: Cumulative snowmelt evolution estimates for 2014, 2015, and 2016. The coloured line represents the median of the 10,000 simulations, while the shaded area represents the interquartile range (25th to 75th percentiles). The vertical black dashed line marks May 1st. We performed a simple snowmelt model using the temperature index equation (Pomeroy and Brun, 2001; Fontrodona-Bach et al., 2025):

Snowmelt (mm of water equivalent) = C_f × (T_air - T_threshold)

where, C_f is the melt factor (mm $°C^{-1}$ day^{-1}), T_air is the daily mean air temperature measured at Scotty Creek, T_threshold is the threshold temperature at which snow begins to melt. T_threshold ranged from -1 °C to +1 °C (Fontrodona-Bach et al., 2025 [preprint], and references therein). C_f was estimated using the relationship between snow density and C_f described by Rango and Martinec (1995). Given that snow density at Scotty Creek ranges from 0.11 to 0.29 (Connon et al., 2021), the corresponding C_f values were estimated to range from 1 mm $°C^{-1}$ day^{-1} to 3 mm $°C^{-1}$ day^{-1}. To account for these uncertainties, we performed 10,000 simulations using a Monte Carlo approach, where C_f and T_thresholds were randomly sampled within their respective ranges.

References**:**

Connon, R.F., Chasmer, L., Haughton, E., Helbig, M., Hopkinson, C., Sonnentag, O., Quinton, W.L., 2021. The implications of permafrost thaw and land cover change on snow water equivalent accumulation, melt and runoff in discontinuous permafrost peatlands. Hydrological Processes 35, e14363. https://doi.org/10.1002/hyp.14363

Fontrodona-Bach, A., Schaefli, B., Woods, R., Larsen, J.R., 2025. [Preprint] Estimating robust melt factors and temperature thresholds for snow modelling across the Northern Hemisphere. https://doi.org/10.5194/egusphere-2025-1214

Rango, A., Martinec, J., 1995. Revisiting the degree-day method for snowmelt computations. J American Water Resour Assoc 31, 657–669. https://doi.org/10.1111/j.1752-1688.1995.tb03392.x

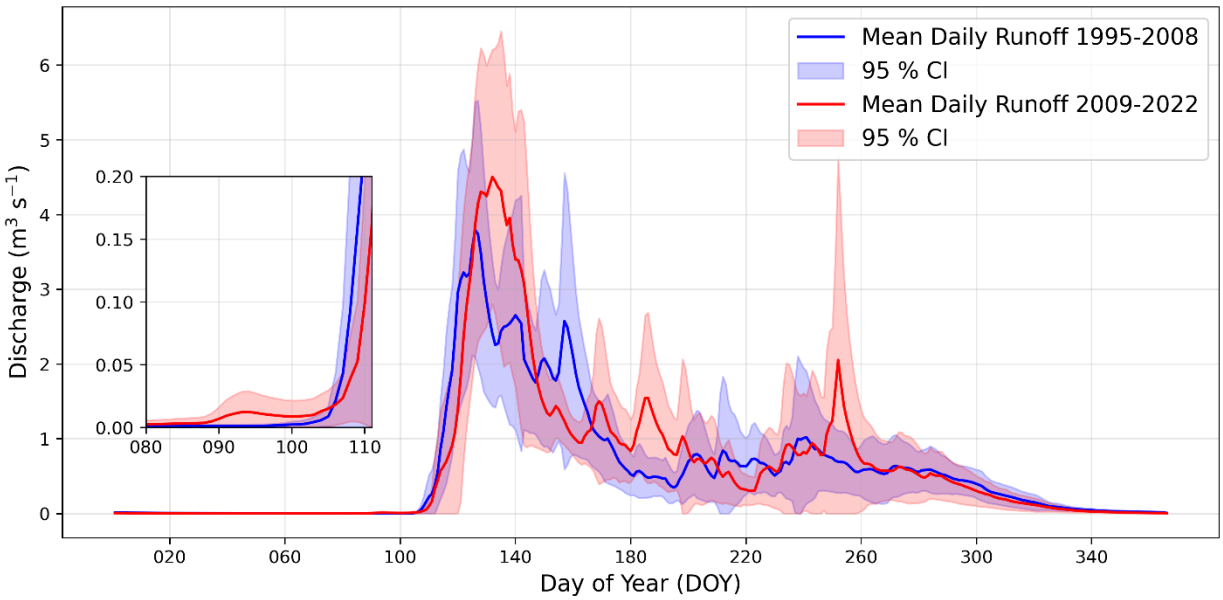

Figure S4: Composite hydrographs for 14-year periods of 1995-2008 and 2009-2022 at Scotty Creek basin outlet. Colored bands correspond to 95 % confidence intervals. The inlet shows a zoom on the spring freshet onset.

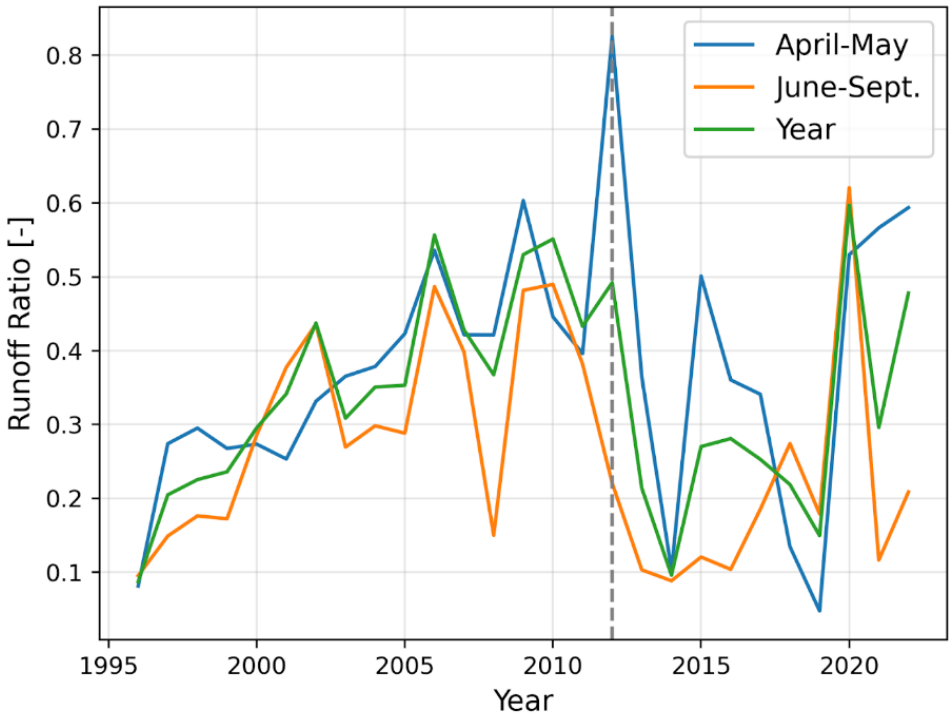

Figure S5: Annual, spring freshet (April–May), and summer (June–September) runoff ratios at Scotty Creek basin. Late-winter snow water equivalent is included in the spring freshet runoff ratio calculation. The dashed vertical gray line corresponds to 2012.

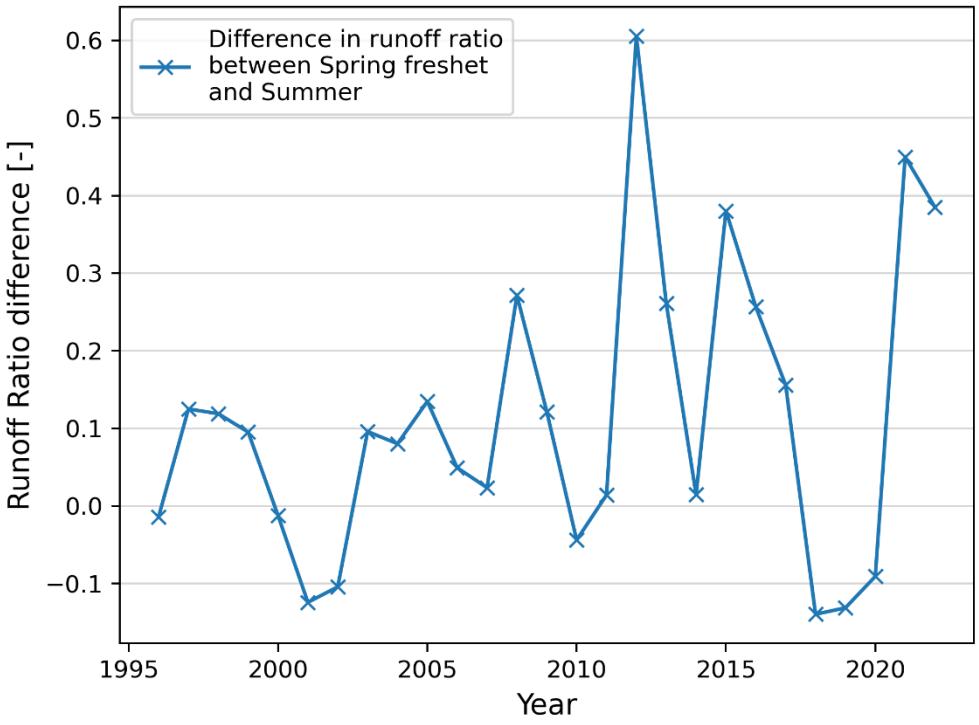

Figure S6: Difference between spring freshet and summer runoff ratios.

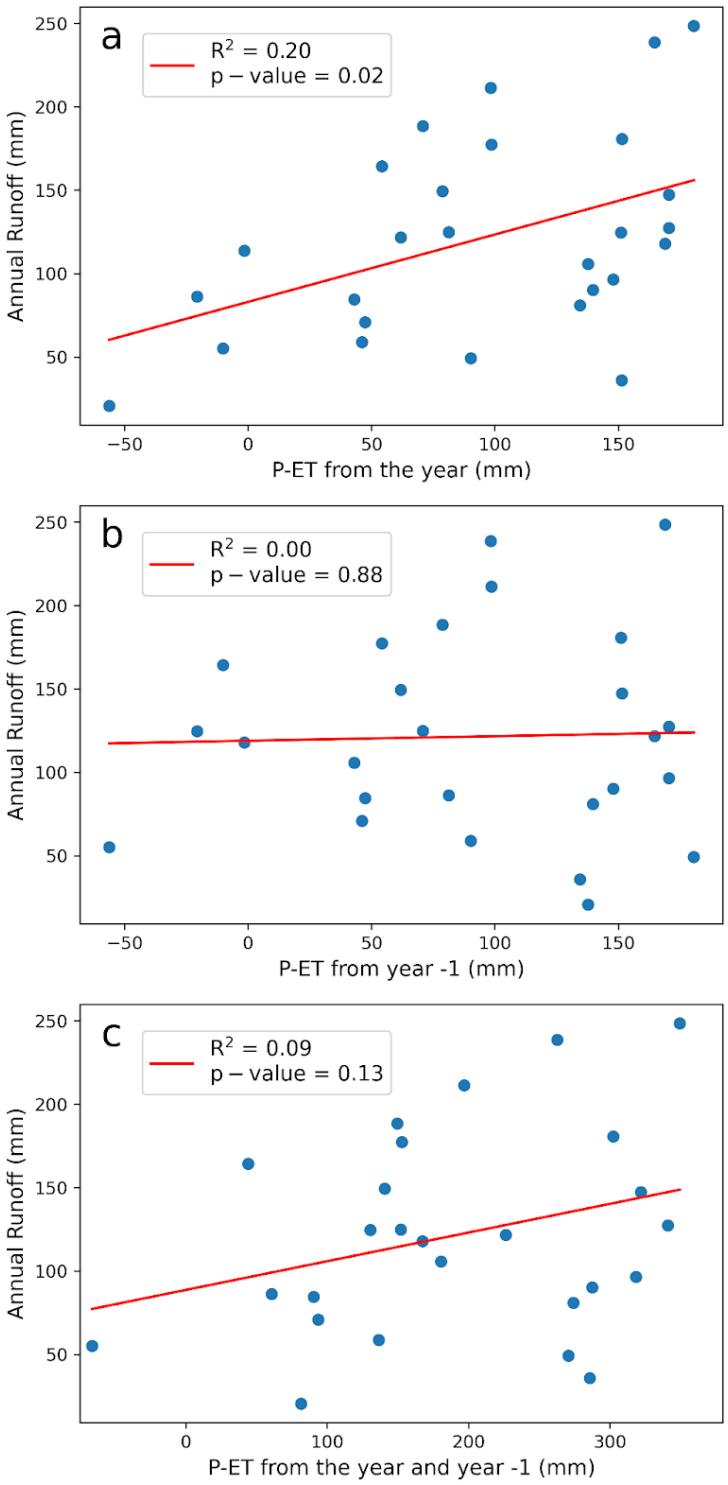

Figure S7: Annual runoff vs. a) current-year effective precipitation, b) previous year's effective precipitation, and c) cumulative effective precipitation from current and previous years. Effective precipitation is defined as precipitation minus evapotranspiration.

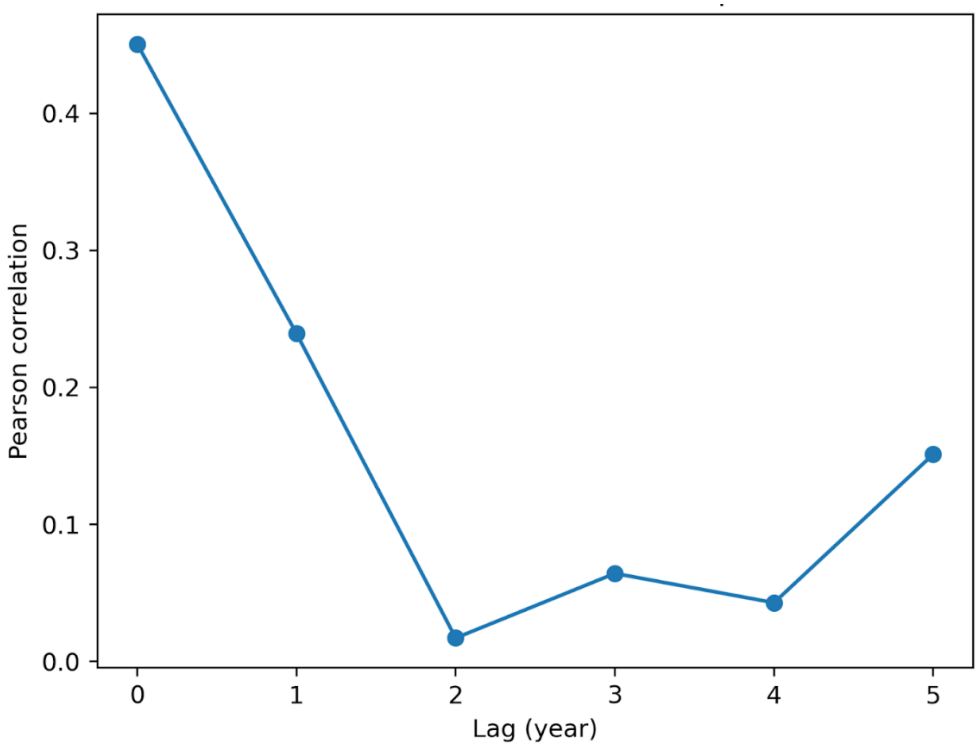

Figure S8: Cross-correlation plot between annual basin runoff and effective precipitation (precipitation minus evapotranspiration).

Supplementary Tables

Table S1. Growing season water balances (May-September, 2014-2016, mm) for the West, East, $East_{FIELD}$ (using the effective field derived sub-basin drainage area, Connon et al., 2015), and South sub-basins at Scotty Creek (Figure 3): snow water equivalent (SWE_{WEST}, SWE_{EAST}, $SWE_{EAST\text{-}FIELD}$ and SWE_{SOUTH}), rainfall ($R_{WEST} = R_{EAST} = R_{SOUTH}$), evapotranspiration ($ET_{LAND} \approx ET_{WEST}, ET_{EAST}, ET_{EAST\text{-}FIELD}$ and ET_{SOUTH}), runoff obtained from discharge measurements (Q_{WEST}, Q_{EAST}, $Q_{EAST\text{-}FIELD}$ and Q_{SOUTH}) and water storage change (ΔS_{WEST}, ΔS_{EAST}, $\Delta S_{EAST\text{-}FIELD}$ and ΔS_{SOUTH}). Potential drainage area was delineated with automated terrain analysis using a digital elevation model (Q_{WEST}, Q_{EAST} and Q_{SOUTH}) and derived from field observations ($Q_{EAST\text{-}FIELD}$). The water balance residual (RES) results from Eq. 1. Wetland water table position (WTP) and discharge data to calculate ΔS_{SOUTH} and Q_{EAST} are not available in 2014 and 2015 (not measured), and 2016 (instrument failure), respectively.

	$SWE_{SUB\text{-}BASIN}$ (mm)	R (mm)	$ET_{SUB\text{-}BASIN}$ (mm)	$Q_{SUB\text{-}BASIN}$ (mm)	$\Delta S_{SUB\text{-}BASIN}$ (mm)	$RES_{SUB\text{-}BASIN}$ (mm)
WEST sub-basin						
2014	102	208	351	4	-159	114
2015	167	316	426	35	-101	122
2016	128	220	442	66	-195	34
EAST sub-basin						
2014	102	208	353	65	-27	-81
2015	169	316	437	74	3	-30
2016	128	220	443	–	-75	–
$EAST_{FIELD}$ sub-basin						
2014	103	208	303	311	-16	-287
2015	172	316	413	358	2	-285
2016	129	220	415	–	-43	–
SOUTH sub-basin						
2014	102	208	384	25	–	–
2015	167	316	452	40	–	–
2016	128	220	460	100	-250	38

Table S2. Growing season monthly (May-September, 2014-2016) water balances (mm month^{-1}) for the West sub-basin (Figure 4): snow water equivalent (SWE_{WEST}), rainfall (R_{WEST}), boreal peatland complex evapotranspiration (ET_{LAND}) approximately corresponding to ET from the West sub-basin ($ET_{LAND} \approx ET_{WEST}$), runoff ($Q_{WEST}$), and water storage change (ΔS_{WEST}). RES_{WEST} indicates the monthly water balance residual resulting from Eq. 1.

2014	SWE_{WEST} (mm)	R_{WEST} (mm)	ET_{WEST} (mm)	Q_{WEST} (mm)	ΔS_{WEST} (mm)	RES_{WEST} (mm)
2014						
MAY	102	20	60	3	-90	149
JUN	0	64	85	0	-8	-14
JUL	0	52	94	0	-38	-4
AUG	0	57	76	0	-1	-17
SEP	0	15	36	0	-21	0
2015						
MAY	167	24	90	15	-90	176
JUN	0	43	114	4	-64	-12
JUL	0	146	94	4	63	-15
AUG	0	47	83	6	-19	-23
SEP	0	55	45	6	9	-5
2016						
MAY	128	36	82	50	-85	117
JUN	0	60	119	11	-54	-16
JUL	0	45	107	2	-58	-6
AUG	0	29	82	1	-35	-19
SEP	0	51	53	2	37	-41

Table S3. Annual (hydrological year [HY]: October-September) water flux components (mm $year^{-1}$) over the period 1996-2022: snow water equivalent (SWE), rainfall (R), precipitation (P), evapotranspiration (ET) from the Breathing Earth System Simulator (BESS) at the basin and basin's headwater portion scales (ET_{BESS_BASIN} and ET_{BESS_HEAD}), runoff (Q_{BASIN_130} and Q_{BASIN_202}), water storage change calculated from the other water flux components (ΔS_{BASIN_130} and ΔS_{BASIN_202}) and runoff ratio (Runoff $ratio_{\_130}$ and Runoff $ratio_{\_202}$). The indices "130" and "202" indicate the surface of the basin in square kilometers.

HY	SWE	R	P	ET $_{BESS\_BASIN}$	ET $_{BESS\_HEAD}$	Q $_{BASIN\_130}$	Q $_{BASIN\_202}$	ΔS $_{BASIN\_130}$	ΔS $_{BASIN\_202}$	Runoff $ratio_{\_130}$	Runoff $ratio_{\_202}$
1995-10 / 1996-09	107	305	412	–	–	46	30	105	122	0.1	0.1
1996-10 / 1997-09	91	304	395	–	–	103	67	31	68	0.3	0.2
1997-10 / 1998-09	95	306	401	–	–	115	74	24	65	0.3	0.2
1998-10 / 1999-09	126	283	409	–	–	123	79	25	69	0.3	0.2
1999-10 / 2000-09	135	297	431	–	–	163	105	8	66	0.4	0.2
2000-10 / 2001-09	107	324	431	–	–	188	121	-18	49	0.4	0.3
2001-10 / 2002-09	181	233	413	262	255	231	149	-79	3	0.6	0.4
2002-10 / 2003-09	119	285	404	253	250	159	103	-8	48	0.4	0.3
2003-10 / 2004-09	96	151	246	267	258	110	71	-131	-92	0.4	0.3
2004-10 / 2005-09	139	215	354	272	270	160	103	-78	-21	0.5	0.3
2005-10 / 2006-09	128	211	339	268	268	241	155	-170	-84	0.7	0.5
2006-10 / 2007-09	116	234	349	270	270	191	123	-112	-44	0.5	0.4

2007-10 / 2008-09	132	199	331	269	267	155	100	-94	-38	0.5	0.3
2008-10 / 2009-09	140	311	450	286	282	305	196	-140	-32	0.7	0.4
2009-10 / 2010-09	82	301	384	285	282	270	174	-172	-76	0.7	0.5
2010-10 / 2011-09	133	277	410	311	306	227	146	-128	-47	0.6	0.4
2011-10 / 2012-09	81	253	334	280	278	210	135	-156	-81	0.6	0.4
2012-10 / 2013-09	106	153	259	269	264	71	45	-81	-56	0.3	0.2
2013-10 / 2014-09	81	134	215	272	271	26	17	-83	-73	0.1	0.1
2014-10 / 2015-09	118	274	392	254	254	135	87	2	51	0.3	0.2
2015-10 / 2016-09	126	175	301	258	257	108	70	-65	-27	0.4	0.2
2016-10 / 2017-09	84	196	280	233	235	91	58	-43	-11	0.3	0.2
2017-10 / 2018-09	90	179	269	223	222	75	48	-29	-2	0.3	0.2
2018-10 / 2019-09	84	246	330	240	237	63	41	27	50	0.2	0.1
2019-10 / 2020-09	96	321	416	236	232	317	204	-137	-24	0.8	0.5
2020-10 / 2021-09	101	298	399	230	230	151	97	18	72	0.4	0.2
2021-10 / 2022-09	127	111	238	239	244	145	93	-147	-95	0.6	0.4

Updated Figure 2:

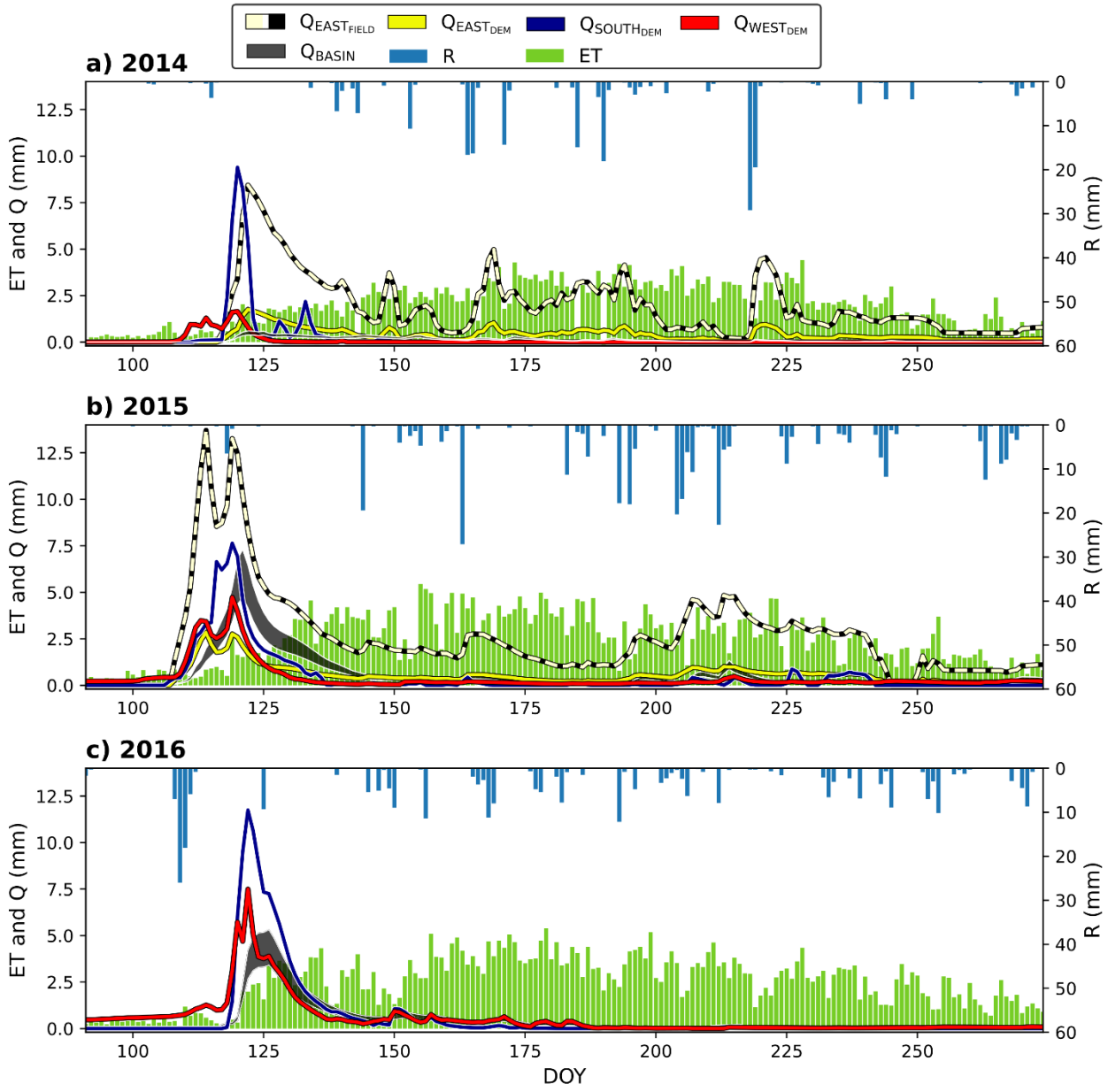

Updated Figure 6: